J. Inst. Eng. India Ser. D (January–June 2023) 104(1):197–203
https://doi.org/10.1007/s40033-022-00391-5

ORIGINAL CONTRIBUTION

Estimation of Filling Property of Cast Al–Si–Mg Alloy

Samavedam Santhi[1] · Jhansi Jadav[1] · P. V. S. L. Narayana[1] · Bhomik K. Deogade[1] · U. S. Jyothi[2]

Received: 2 June 2022 / Accepted: 29 July 2022 / Published online: 16 August 2022

Abstract Cast Al-Si-Mg alloys find broad applications in automobile components. Manufacture of defect free castings especially for long thin walled structures requires understanding of filling property. The filling property of cast alloy is studied using pin test piece through cylindrical cores for simulation followed by validation studies. Coating on the mould, pouring temperature and sand fineness are considered as parameters for this study. Simulation studies have been carried out using design of experiments. Results of casting simulation are in good agreement with validation studies. The parameters providing highest filling property are graphite coat on mould, AFS sand fineness 40 and pouring temperature with + 20 °C for simulation and validation studies.

Keywords Cast Al-Si-Mg alloy · Filling property · Simulation · Mould coat · Pouring temperature

Introduction

The traditional method of metal casting is the sand casting as most of the castings are developed using this process [1]. The most often used alloying element in Aluminium alloy castings is Silicon, which improves castability by increasing fluidity, hot tear resistance and fine strength [2–4]. The primary Si is having higher amount of latent heat, which in turn increases the solidification time of the liquid alloy during solidification, this leads to the improvement in the fluidity of the corresponding alloy. [5]. Magnesium (Mg) addition to this alloy improves mechanical properties by forming a metastable precipitate of Mg_2Si during age-hardening treatment [6].

Lubos Pavlak cited that mould filling property of molten metal plays a major role on the quality of casting [7]. It is the ability of the cast alloy to replicate the proportions and contours of the cavity of the mould completely. Mould filling property involves viscous flow of the molten metal with numerous momentary permitted surface boundaries [8] besides entire filling of long lean castings [9]. The mould filling property is a molten alloy flow at variable temperature accompanied with heat dissipation to the surroundings and solidification [10]. A pin test piece for the calculation of the above said characteristic has been designed by Engler and Ellerbrok [11–13]. Coating on the mould, Pouring temperature, Fineness of the sand, Alloy composition, Pressure head and Wall thickness are the factors which are influencing the mould filling property [13, 14].

Simulation

Experimental design has been done using the MINITAB [15]. Coat on the mould promotes smooth flow by influencing surface tension and there by changing the solidification rate. Flemings, et al. stated that when drop in surface tension is observed, there is rise in pressure head in the molten metal, resulting in increased mould filling property [4, 16, 17]. Additional heat energy is removed from the forwarding molten alloy front prior to it commences to solidify, due to rise in the pouring temperature of the molten metal. Table 1 is providing the particulars corresponding to the 3 variables

✉ Samavedam Santhi
santhi_samave@yahoo.com

[1] Mahatma Gandhi Institute of Technology, Hyderabad, India

[2] Gokaraju Rangaraju Institute of Engineering and Technology, Hyderabad, India

Table 1 Variables and corresponding levels for the study

	Variable 1 fineness of the sand (AFS No.)	Variable 2 coating on the mould	Variable 3 pouring temperature (°C)
Level 1	25	Graphite	PT
Level 2	40	No coating	PT + 20

and 2 levels and Table 2 is presenting the Orthogonal array of L4 (2**3) for this study.

Solid Model

Figure 1 is giving the details of the dimensions and solid model forfilling property. Filling property of the cast Al-Si-Mg alloy (US A 356) is calculated by pin test section through cores of cylindrical shape [11, 12], and the calculation of the diameter of meniscus of molten metal immediately at the time of freezing. For the present study, ϕ50mm cylindrical cores are considered.

Simulation Studies

The simulation studies have been conducted through Finite Difference Method (FDM)-based software. Simulation creates a virtual environment for casting solidification, predicting and analysing the quality of the cast components. The input data for the simulation studies are solid model of the casting, material properties and boundary conditions. The material properties considered are specific heat, thermal conductivity, density, interfacial heat transfer coefficient, pouring temperature of the molten metal and initial temperature of the mould. The simulation outcomes are given as contour graphs of solid fraction, time of solidification and freezing rate.

Table 2 L4 Orthogonal array for the present studies

Exp no	Fineness of the sand (AFS No.)	Coating on the mould	Pouring temperature, PT(°C)
1	25	Graphite (GC)	PT + 20
2	25	Graphite (GC)	PT
3	25	No coating (NC)	PT + 20
4	25	No coating (NC)	PT
5	40	Graphite (GC)	PT + 20
6	40	Graphite (GC)	PT
7	40	No coating (NC)	PT + 20
8	40	No coating (NC)	PT

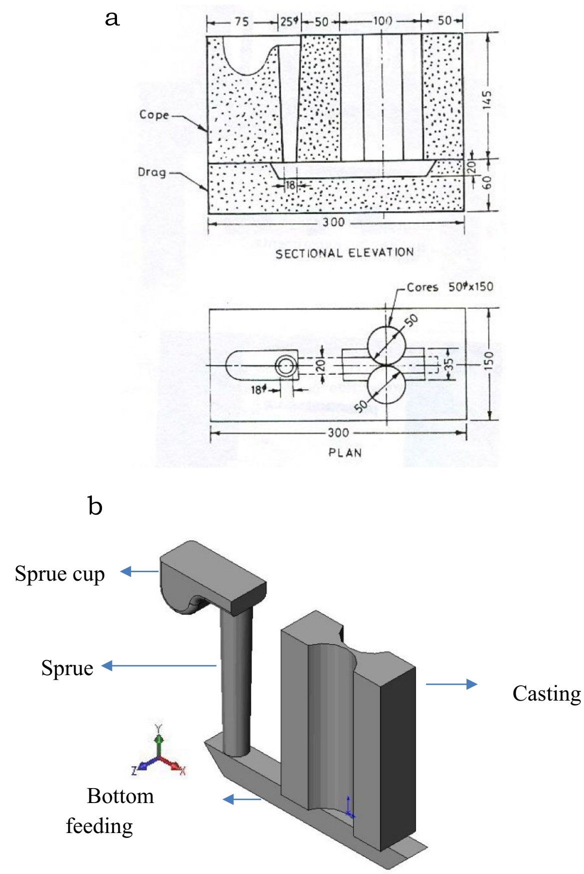

Fig. 1 **a** and **b** Dimensions and solid model

For accurate results, the simulation studies require introduction of boundary conditions. The boundary condition values to be described at the beginning of the process are thermal data of metal and casting mould, conditions of heat exchange between a casting and individual parts of mould and between mould and surroundings.

The interfacial heat transfer coefficient (h) is the rate of heat loss through the metal/mould interfaces which influence the filling property and shrinkage or volume deficit characteristics. However, interfacial heat transfer coefficient is not a simple material property and is dependent on chemical, physical interfacial conditions, mould and casting material properties and casting geometry.

The thermal data of the alloy and sand mould, conditions of heat transfer between the alloy and discrete parts of the mould and among the mould and its environment are the provided as the boundary conditions for the simulation. Interfacial heat transfer coefficient is depending on casting geometry, physical–chemical interfacial conditions, thermo-physical properties of mould and alloy. In the present studies, interfacial heat transfer coefficient values for conformity of simulation and the experimental studies are consistent. The properties of silica sand and cast alloy for the present study [18–20] are given in Table 3.

The solid model, has to be introduced in the stereo lithographic (stl) format (Fig. 1b) as the solution zone and with a distinct identification of each material. Boundary conditions are allocated at mould, alloy and mould coat interfaces.

Cast Al-Si-Mg alloy is long freezing range alloy the flow of liquid alloy stops, when the amount of fraction of solid is in the range of twenty-five to fifty percent in the present alloy [21–23]. During the solidification of an alloy, the dendrite coherency point at which the discrete dendrites start impinging upon their neighbours [23, 24], a solid structure forms and accordingly the liquid metal flow is freezed.

From literature [23–26], that the dendrites start interrupting and form a solid network that stop further liquid alloy flow at a 30% fraction of solid and which corresponds to a coherency temperature, Tc of 873 K for the present alloy.

Results of Simulation Studies

The output of the simulation is cooling rate and fraction of solid. The Leaving solid fraction is the total fraction of solid at which the solver leaves and it is corresponds to fraction solid of 30%. Simulation studies of casting obtained for one of the experiment is shown in Fig. 2.

Simulation studies are conducted as per Table 2 and values can be obtained at pressure heads and measurement of the diameter of meniscus of liquid alloy immediately at the time of freezing in the casting. The molten alloy poured into the sprue raises in the mould cavity and fills the curved cavity connecting the two cores of cylindrical shapes having a line connection at the centre, then freezes beforehand completely filling the casting as given in Fig. 2.

Calculation of Mould Filling

The reverse of the diameter of curvature of the edge tip of the formed fin is giving the value of the mould filling property.

Table 3 Data for simulation studies

S. no	Parameter	US A356	Sand
1	Melting point, (°K)	934	–
2	Thermal conductivity, W/mm.K	0.159249	90.27×10^{-5}
3	Density (Kg/m^3)	2680	1522
4	Liquidus temperature (°K)	886	–
5	Solidifying range (°K)	400	–
6	Latent heat of fusion, J/kg	388,442	–
7	Specific heat, J/kg.K	962.944	1076.007
8	Interfacial Heat Transfer Coefficient, HTC, W/m^2 K		
9	Metal—mould	35×10^{-4}	
	Metal—coating mould	15×10^{-4}	

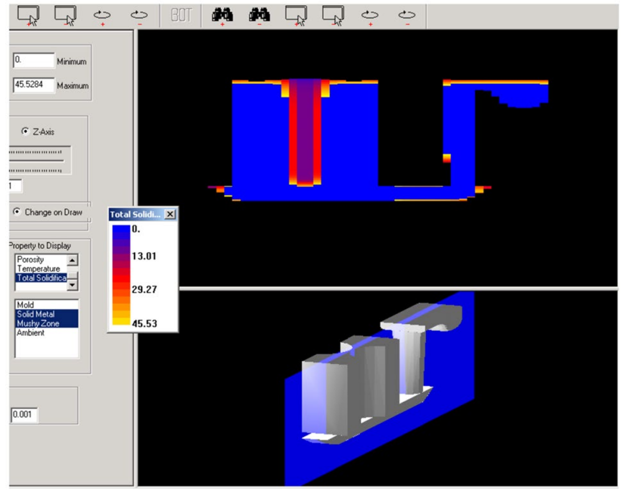

Fig. 2 Simulation studies

The diameter at the tip of the formed fin gives the meniscus diameter (2r = d) of the molten alloy at the time of solidification as represented in Fig. 3 for one particular pressure head. It is difficult to measure the diameter of the formed fin tip and it is calculated using the formula as shown in Fig. 3.

As per Fig. 3

$$R^2 + (r + x)^2 = (r + R)^2 \quad (1)$$

so 1/d = (R-x) /x^2, R = radius of the sand core, mm, r = radius of the meniscus (2r=d), mm, 2x = distance between

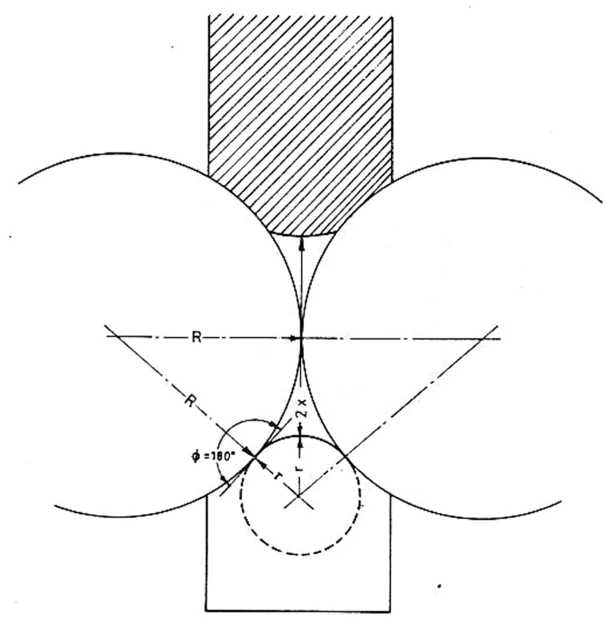

Fig. 3 Measurement of mould filling property

edges, mm, 1/d = mould filling ability, 1/mm Distance between two fins

Images of the contour plots of the distance between two fins are changed to solid model. 3D solid works software is used for generating 3D model and Fig. 4 is displaying for one of the experiment (as given in Table 2) at different pressure heads from the bottom for every 5 mm pressure head interval till it is 95 mm. The mould filling ability values for remaining simulation experiments are calculated and tabulated in Table 4.

Influence of Pressure Head

Metallostatic pressure increases with rise in elevation of the sprue. The filling property of the solidified casting is expressed as the reciprocal of the diameter of the meniscus of formed fin tip. Figure 5 shows the effect of pressure head on filling property of the alloy. Rise in pressure head leading to rise in the metallostatic force, allowing the molten alloy to enter the finer contours between the cores thus dropping the formation of fin edge and rise in the filling property. The molten alloy has to be in contact with larger area in order to penetrate into mould cavity which promotes faster freezing, because of rise in pressure head.

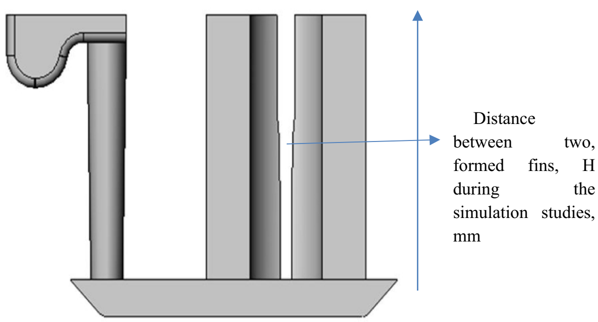

Fig. 4 3D image

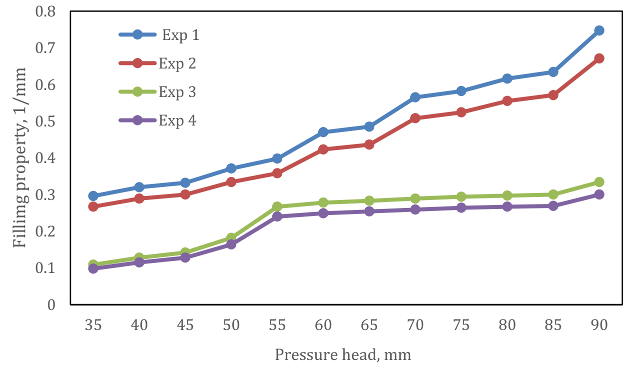

Fig. 5 Influence of pressure head

Influence of Graphite Coat

To minimise the friction among the surfaces of alloy and mould, the mould exterior is coated with graphite. Mould coat is providing a protecting outcome during heat transmission and so dropping the rate of cooling in the liquid alloy. So the molten alloy is in the fluid state for extended time and fills the whole mould cavity. Graphite coat generates a smooth alloy and mould interface which is providing the minimum resistance to fill the fine contours, thereby increasing the mould filling property (as shown in Fig. 6).

Influence of Fineness of the Sand

The filling property rises with rise in fineness of the sand (Fig. 7). The fine sand shows better mould filling property. Coarse sand is having the faster heat dissipation rate to the

Table 4 Simulation Results for 8 simulation experiments

H,mm	1/d, 1/mm							
	1	2	3	4	5	6	7	8
35	0.296	0.267	0.109	0.098	0.516	0.465	0.102	0.100
40	0.320	0.289	0.128	0.115	0.565	0.508	0.108	0.101
45	0.332	0.300	0.142	0.128	0.582	0.524	0.182	0.164
50	0.371	0.334	0.182	0.164	0.599	0.539	0.191	0.171
55	0.398	0.358	0.267	0.240	0.665	0.587	0.227	0.204
60	0.470	0.423	0.278	0.249	0.671	0.603	0.278	0.249
65	0.485	0.436	0.283	0.254	0.689	0.620	0.334	0.300
70	0.565	0.508	0.289	0.259	0.767	0.689	0.396	0.355
75	0.582	0.524	0.294	0.264	0.787	0.707	0.436	0.391
80	0.616	0.555	0.297	0.267	0.893	0.802	0.450	0.404
85	0.634	0.571	0.300	0.269	1.128	1.012	0.465	0.416
90	0.747	0.671	0.334	0.300	1.398	1.252	0.479	0.429

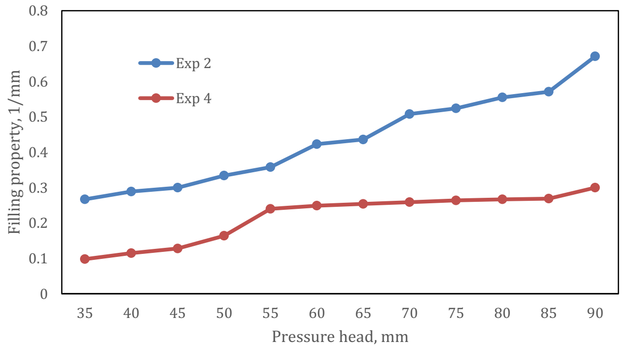

Fig. 6 Influence of graphite coat

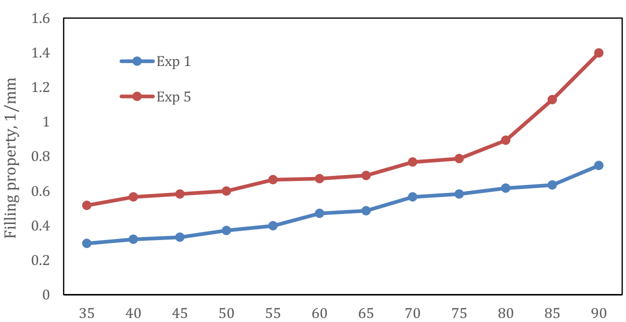

Fig. 7 Influence of sand fineness

surroundings than the fine sand and solidifies the alloy faster. This restricts the filling up of the cavity contours between the sand cores and reduces the filling property.

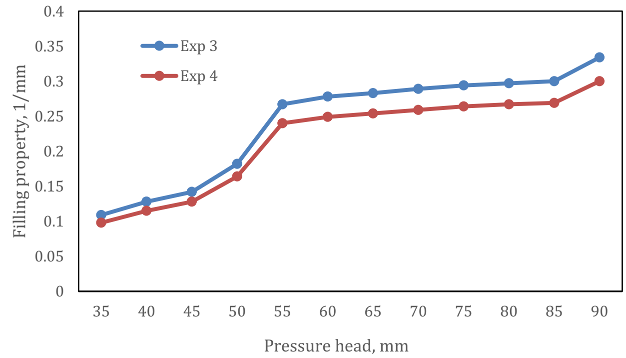

Fig. 8 Influence of pouring temperature

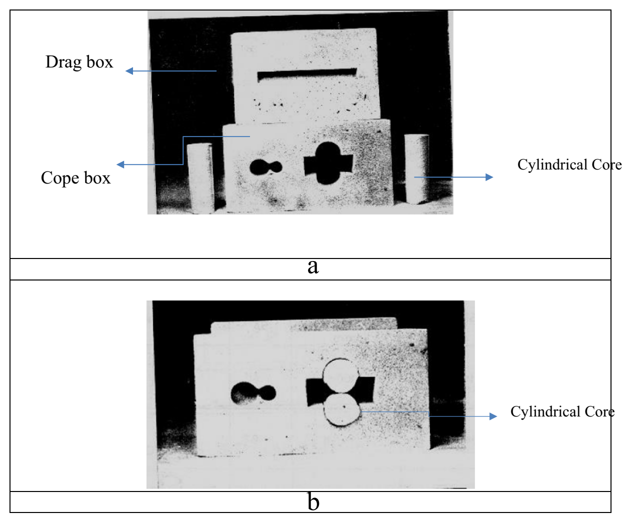

Fig. 9 Tooling for validation experiments

Influence of Pouring Temperature

Rise in pouring temperature of the molten alloy increases the heat content of the alloy, resulting in alloy being molten state for lengthier period. This is promoting the metallostatic pressure head to act on the liquid alloy for a longer period of time, thus forcing the alloy to easily enter and reproduce fine outlines, leading to increase in filling property as shown in Fig. 8.

Consequently, the molten alloy easily go in the cavities among the cores and is filling the complete mould cavity. For low pouring temperatures fractional freezing is occurring during pouring of liquid metal into the mould cavity. Higher pouring temperature delays the nucleation and growth of the solidification at the tip of the flowing molten metal in the mould cavity, there by filling ability increases, driving the molten metal to easily enter and replicate outlines.

Experimental Studies

Without validation experiments it is difficult to realize the outcomes obtained by simulation are realistic, hence four validation experiments are conducted (1, 4, 5 and 8 of Table 2) and process Variables studied are same as simulation studies.

Green Sand Mould

Drag box, cope box and cores and complete mould for the validation experiments are given in Fig. 9 [26, 27]. Green sand moulds are set with proper ramming and 5% Bentonite and 7% water of sand weight are considered as sand binders. The permeability of the green sand mould is 450, green compression strength is 800 g/cm^2 and mould hardness is 75 on B scale. For mould coatings, the graphite dye is sprayed

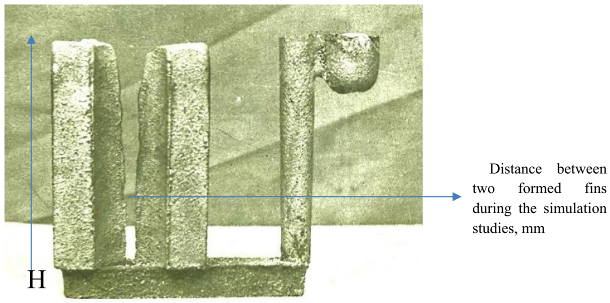

Fig. 10 Solidified casting

on to the sand mould and dried instantaneously by lightening a flame on the sprayed mould exterior.

Melting and Pouring

The Al-Si alloy is melted in an electric resistance furnace with a mild steel crucible of 20 kg capacity and temperature is measures using a thermocouple. The molten alloy is tapped into a ladle for pouring into the mould cavity. Ladle is carrying the liquid metal from furnace and the pouring height is kept steady to avoid turbulence during pouring. Figure 10 shows the solidified casting.

Results

Calculation methodology considered for the validation experiments results is as of Fig. 3 and Eq. 1. To mark the height for every 5 mm distance, Height gauge is considered and the gap between the fin edges 2 × is measured with vernier micrometer [21, 27] is used and is given in Table 5, as shown in Fig. 10. The filling ability values are given in Table 6.

Table 5 Distance between the fin edges, 2 × (mm)

H,mm	Distance between the fin edges, 2 × (mm)			
	1	2	3	4
35	5.4	3.7	7	3.4
40	5.9	3.8	7.3	3.5
45	5.7	4	7.4	4.5
50	6	4.5	7.5	4.6
55	6	5.5	7.8	5
60	6.7	5.5	7.9	5.5
65	6.8	5.55	8	6
70	7.6	5.6	8.5	6.5
75	7.3	5.65	8.5	6.8
80	7.6	5.68	9	6.9
85	7.7	5.7	10	7
90	8.3	6	11	7.1

Table 6 Results for validation studies

H,mm	1/d, mm^{-1}			
	1	2	3	4
35	0.326	0.147	0.569	0.124
40	0.394	0.156	0.624	0.131
45	0.366	0.174	0.643	0.220
50	0.409	0.220	0.662	0.233
55	0.410	0.330	0.721	0.278
60	0.518	0.338	0.741	0.339
65	0.535	0.346	0.762	0.409
70	0.648	0.353	0.871	0.485
75	0.650	0.359	0.882	0.535
80	0.681	0.364	0.987	0.550
85	0.804	0.366	1.225	0569
90	0.826	0.409	1.552	0.587

Comparison of Results

The results of simulation are in accordance with validation studies. The correlation co-efficient is calculated to ascertain the association among the two results using the formula, and it is given in Table 7 for experiment no.3.

Correlation(r) = [(PΣcd—(Σc)(Σd))/Sqrt([PΣc^2—$(\Sigma c)^2$][PΣd^2—$(\Sigma d)^2$])].

P = number of values (varying pressure head, H from 35 to 90 mm).

c = Filling ability values for simulation.

d = Mould filling values for experimental studies.

In the present study the correlation coefficient value nearing + 1, hence representing good correlation. The Correlation Co-efficient for four experiments are calculated and are

Table 7 Correlation co-efficient for filling ability values

P	c	d	c x d	c^2	d^2
35	0.4650	0.5697	0.264911	0.216225	0.324558
40	0.5089	0.6240	0.317554	0.258979	0.389376
45	0.5240	0.6427	0.336775	0.274576	0.413063
50	0.5394	0.6617	0.356921	0.290952	0.437847
55	0.5871	0.7208	0.423182	0.344686	0.519553
60	0.6036	0.7412	0.447388	0.364333	0.549377
65	0.6203	0.7619	0.472607	0.384772	0.580492
70	0.6897	0.8708	0.600591	0.475686	0.758293
75	0.7077	0.8818	0.62405	0.500839	0.777571
80	0.8021	0.9878	0.792314	0.643364	0.975749
85	1.0123	1.2250	4.636291	3.754414	5.725879
90	1.2528	1.552	1.944095	1.569508	2.408083

equal to 0.991, 0.985, 0.992 and 0.991, indicating a strong co-relation between the two studies.

Conclusions

In the present study more than 0.9 correlation co-efficient results are observed and it is representing a good correlation between the simulation and validation studies. Filling ability value for simulations is quantified using the three-dimensional solid works program. Mould coat using the graphite, AFS sand fineness number 40 and pouring temperature T + 20 °C are the process parameters providing optimum filling ability value for simulation and validation studies.

Funding The authors have not disclosed any funding.

Declarations

Conflict of interest The authors declare that they have no known competing financial interests or personal relationships that could have appeared to influence the work reported in this paper.

References

1. E.P. Degarmo, J.T. Black, R.A. Kohser, *Materials and processes in manufacturing* (Wiley, New York, NY, 2003)
2. M. Di Sabatino, L. Arnberg, Castability of aluminium alloys. Trans. Indian Ins. Metals **62**(4), 321–325 (2009)
3. Foseco Non-Ferrous Foundry man's Handbook2008 Eleventh edition, Revised and edited by Butterworth Heinemann publisher John R. Brown
4. F.R. Mollard, M.C. Flemmings, E.F. Nyama, Understanding aluminium fluidity: the key to advanced cast products. AFS Trans **95**, 647–652 (1987)
5. K.R. Ravi, R.M. Pillai, K.R. Amaranathan, B.C. Pai, M. Chakraborty, J. Alloys Compd. **456**, 201–210 (2008)
6. M.T. Di Giovanni, E. Cerri, T. Saito, S. Akhtar, P. Asholt, Y. Li, M. Di Sabatino, How slight solidification rate variations within cast plate affect mechanical response: a study on As-Cast A356 Alloy with Cu additions. Adv. Mater. Sci. Eng. (2018). https://doi.org/10.1155/2018/4030689
7. L. Pavlak, Effect of filling conditions on the quality of cast aluminum cylinder heads. MJOM J. Metall. **14**(3), 31–39 (2005)
8. Barkhudarov MR, Williams K, Simulation of surface turbulence, fluid flow during mold filling. Trans AFS Foundry Soc; 95–90 and 669–674 (1995)
9. S.U. Yanqing, Tiejun Zhang, G.U. Jingjie, Hongsheng Ding, B. Weisheng, Jun Jia, F.U. Hengzhi, Physical simulation of mould-filling processing of thin-walled castings under traveling magnetic field. J. Mater. Sci. Technol. **20**(1), 27–30 (2004)
10. S. Engler, R. Ellerbrok, Ueber des formfullengsvermoegen, Giess, Forsch, p49, 1974
11. S. Sundarrajan, H.D. Roshan, Studies on mould filling ability characteristics of Mg-Al Alloys. Trans. Am. Foundrymen Soc. **97**, 607–616 (1989)
12. H. Yan, W. Zhuang, Y. Hu, Q. Zhang, H. Jin, Numerical simulation of AZ91D alloy automobile plug in pressure die casting process. J.Mater. Process. Technol. **187**(5), 349–353 (2007). https://doi.org/10.1016/j.jmatprotec.2006.11.186
13. B. Ravi, Casting method optimization driven by simulation. Metals Miner. Rev. **34**(3), 39–43 (2008)
14. M.C. Flemings, Fluidity of Metals – techniques for producing ultra-thin section castings. British Foundryman **57**, 312–325 (1964)
15. Minitab 16, User Manual of MINITAB, 2008, www.minitab.com
16. N. Chvorinov, Theory of the solidification of castings. Geisserei **27**, 177–225 (1940)
17. M. Trovant, A Boundary condition coupling strategy for the modeling of metal casting processes, National Library of Canada, Acquisitions and Bibliographic Services, (1998)
18. M. Venkataramana, V. Vasudeva Rao, R. Ramgopal Varma, S. Sundarrajan, Instrumentation to measure heat transfer coefficient at the metal mold interface. J. Instrum. Soc. India **37**(3), 157–163 (2008)
19. G.S. Cellini, L. Tomesani, Metal head - dependent HTC in sand casting simulation of aluminium alloys. J. Achiev. Mater. Manuf. Eng. **29**(1), 47–52 (2008)
20. S. Santhi, Modeling and Simulation of Flow and Fill characteristics of non ferrous alloys, PhD Thesis submitted to JNTUH, Hyderabad, August 2012
21. M. Di Sabatino, L. Arnberg, F. Bonollo, Simulation of Fluidity in Al-Si alloys, Metallurgical Science and Technology, Ed. by Teksid Aluminum, July (2005), 23(1): 3–10
22. ASM Metals Handbook Volume 15, Casting, ASM International, The Materials Information Company (2004)
23. J. Campbell, The new of cast metals, Castings, Butterworth-Heinemann, Secondedition (2003)
24. L. Arnberg, L. Bäckerud, and G. Chai: Solidification characteristics of aluminium alloys Vol 3, Dendrite Coherency, AFS, Des Plaines, IL (1996)
25. John Campbell, R.A. Harding, *TALAT Lecture 3205: The fluidity of molten metals, prepared by IRC in materials* (The University of Birmingham, England, 1994)
26. S. Santhi, S.B. Sakri, D. Hanumantha Rao, S. Sundarrajan, Mould filling ability characterisation of cast aluminium alloys using design of experiments. J. Metall. (2012). https://doi.org/10.1155/2012/624650
27. S. Santhi, U. S. Jyothi, and K. Srinivasa Vadayar, Calculation of filling characteristics of cast Al-Si alloy, in: Recent Advances in Manufacturing, Automation, Design and Energy Technologies Proceedings from ICoFT 2020, Lecture Notes in Mechanical Engineering (LNME), pp 47–56, DOI: https://doi.org/10.1007/978-981-16-4222-7_6